Int. J. Solids Structures, 1972, Vol. 8, pp. 613 to 626. Pergamon Press. Printed in Great Britain

ANALYSIS OF A BOX MADE OF ELASTIC ORTHOTROPIC PLATES

J. R. YALAKKI† and A. S. D. WANG

College of Engineering, Drexel University, Philadelphia, Pennsylvania 19104

Abstract—Elastic stresses, deflections and critical pressures for various modes of failure of a rectangular box placed in a uniform external pressure field are analyzed by a classical linear plate theory. The field equations governing the deflection of an orthotropic plate are solved by means of a superposition scheme and a method of single series expansion. The over-all solution for the entire box is arrived at by imposing continuity conditions at the edges where the individual plates meet. The method of analysis presented here is also adaptable to boxes on which external compressive loads are not uniformly distributed, but are self-equilibrating.

INTRODUCTION

THE analysis of thin walled boxes subject to the action of applied loads is important in the design and construction of such structural members as aircraft wing sections, deep-sea vessel compartments, box-girders used in bridges, modern cargo containers and various other types of structural boxes which are subjected to either internal or external loads.

Boxes made of elastic isotropic panel plates and subjected to static internal pressure have been studied by Conway [1], who utilizes a linear plate theory and treats the panels as simple bending members. From a structural point of view, the behavior of a box under external compressive load differs fundamentally from that of the same box pressurized within. The phenomenon of structural instability is usually predominant in the former case.

The purpose of the present work is to study the strength and stability of rectangular boxes that are made of orthotropic panel plates and are placed in a uniform external pressure field. The principal planes of elastic orthotropy of the panels are assumed parallel to the edges of the box. This assumption, though restrictive, accommodates such box panels as rib-reinforced plates, cross-ply fiber-reinforced laminates, sandwich plates etc., as long as their over-all elastic properties may be represented and described by a homogeneous orthotropic plate. A linear classical plate theory [2, 3] is used to analyze individually each panel of the box. The method of solution is based on a scheme of superposition and a Fourier series expansion. Specifically, we assume for each of the six panels forming the box, a finite Fourier series for the unknown edge moments. Furthermore, in view of the small deflection assumption made in the linear theory, it is also assumed that the edges of the box will remain straight throughout the loading history. The panels may then be regarded as being simply supported along all edges and being acted upon by a uniform normal pressure and all-round edge moments with the presence of in-plane edge forces. These forces are transmitted from the transverse edge shears of the neighboring side panels of the box. The distribution of the edge forces is assumed to be uniform along the edges. In this manner, field solutions concerning the stresses, moments as well as deflections of each of the panel plates may be obtained in terms of the Fourier coefficients appearing in the

† Now at: Day and Zimmermann, Inc., Philadelphia, Pennsylvania.

finite edge moment series. These coefficients are finally determined by requiring rigid edge rotations of the total structure. Some remarks about the convergence of the series solution scheme are also included.

Since the box, when possessing certain symmetry, exhibits a multi-degree of freedom in deflection, it becomes necessary to determine all possible modes of failure and the corresponding stresses and deflections up to the failure load. This is accomplished here first by analyzing the stability of the structure which yields all modes of buckling and the corresponding buckling pressures. Secondly, we perturb the geometric symmetry of the box so as to obtain all field informations prior to the occurrence of instability failure. Numerical results are presented to illustrate these aspects.

Effects of orthotropic reinforcements are also discussed by means of numerical examples. Significant improvement in the strength of the box may be achieved by proper reinforcement and the selection of physical dimensions. This latter observation suggests the possibility of an optimal design for the structure.

ANALYSIS

We shall consider a rectangular box of sides L, aL and bL; and the box is subjected to a uniform hydrostatic pressure q, Fig. 1(a). Three pairs of thin elastic plates, whose macrophysical properties are assumed orthotropic, are joined rigidly at their edges. The thickness and the material properties of any pair may be different from those of the other pairs, but

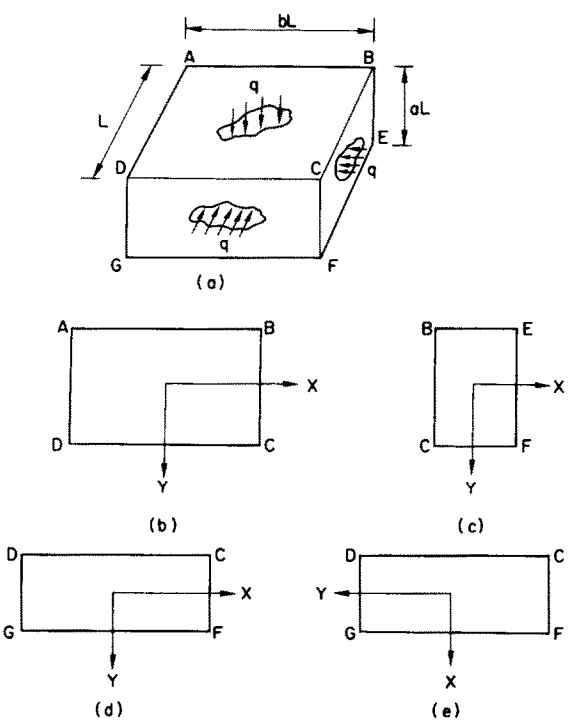

FIG. 1. Isometric view of box and panels.

each pair must consist of two identical plates. Because of this symmetry, only the top, side and the front plates will be considered in the analysis. Figures 1(b)–(d) show the local coordinates for the three plates, respectively. Figure 1(e) shows an alternative coordinate system for the front plate. The latter is necessary because of the matching conditions which will be applied later. In view of the small deflection assumption, as was discussed earlier, each of the three plates may be regarded as being simply supported along all edges and being acted upon by in-plane edge forces P and edge moments M, Fig. 2. The exact distribution of the edge forces and moments is not yet known.

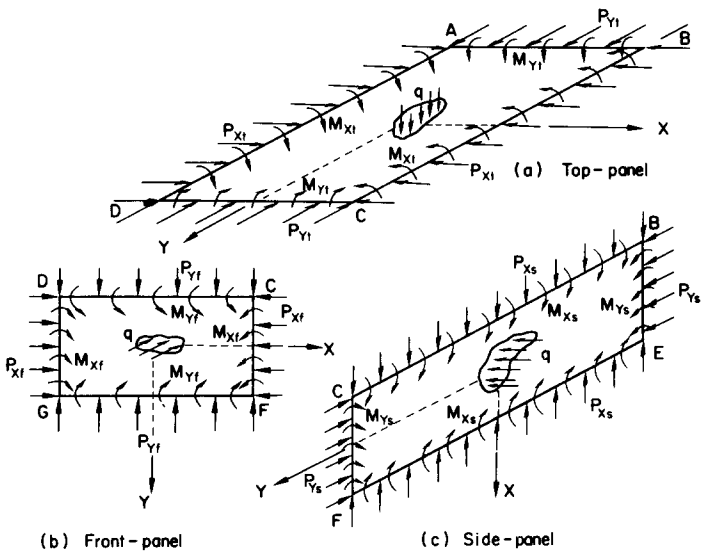

FIG. 2. Free-body diagrams of panels (simple supports and twisting moments along edges are not shown).

There exist twisting moments along the edges as well, but these are not shown in Fig. 2. These moments are self-equilibrated resulting in an equivalent concentrated reaction at the four corners of the plate. These corner reactions are in static equilibrium when the entire box is considered.

Representation of in-plane edge forces

Representing the in-plane edge forces of each plate, we first note that the edge forces are transmitted from the transverse edge shears of the neighboring side panels of the box. The distribution of these shear forces is an unknown unless total solutions of the entire structure are obtained. In what follows, we simply assume that the edge forces are uniformly distributed along the edges and their intensity are calculated by multiplying an appropriate area such as shown in Fig. 3, by the pressure q. For example, the total edge force along BC of the top panel is $P_{Xt}L = q$ (area $CJKB$); along CD of the top panel is $P_{Yt}(bL) = q$ (area $CDMN$), etc. Thus the six edge forces on the top, side and front plates are given by

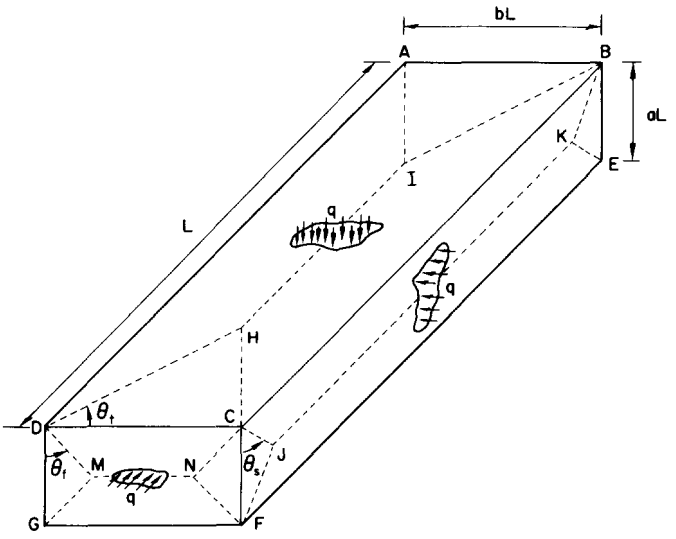

FIG. 3. Diagram showing partitions of edge force transmission.

(in force per length),

$$P_{Xt} = aqL(2-a\tan\theta_s)/4 \qquad P_{Ys} = aqL\tan\theta_f/4$$

$$P_{Yt} = aqL\left(2-\frac{a}{b}\tan\theta_f\right)\Big/4 \qquad P_{Xf} = aqL\tan\theta_s/4 \tag{1}$$

$$P_{Xs} = bqL(2-b\tan\theta_t)/4 \qquad P_{Yf} = bqL\tan\theta_t/4.$$

All quantities indexed by t, s or f are associated respectively to the top, side or the front plate.

The angles θ_t, θ_s and θ_f must be appropriately valued so as to yield a close agreement between the edge forces now assumed and those later computed. In general, these angles depend on the rectangularity of the box. For example, when $a = b = 1$, i.e. a cubic box, $\theta_t = \theta_s = \theta_f = \pi/4$. If $a \neq b \neq 1$, the angles must be determined by a trial-and-iterate process. Briefly, the process begins with assuming $\theta_t = \theta_s = \theta_f = \pi/4$. The edge forces are then calculated according to equations (1). These will be used in the solution for the field equations of each of the plates which, after the matching of the edge conditions, furnish the values of the transverse shear forces along the edges of each plate. The resultant of the shear on any edge is redistributed uniformly and is compared with the initially calculated corresponding edge force. If a close agreement is not obtained, a new trial based on the newly computed edge shear is repeated again until a satisfactory agreement is reached†.

Representation of edge moments

As for the unknown edge moments, their expressions are here assumed a type of Fourier half-range cosine series. Again, because of the symmetry, only the moments along the

† In the numerical work reported in this note, the iteration usually requires no more than three or four trials in order to achieve an agreement within 0·1 per cent. For details, see [4].

longitudinal, vertical and the horizontal edges are considered. For the coordinate systems shown in Fig. 1, the moments along AD, BC and EF are, respectively,

$$M_X = \sum_{m=1,3,\ldots}^{\infty} E_m \cos\frac{m\pi Y}{L} \qquad X = \pm bL/2$$

$$M_Y = \sum_{m=1,3,\ldots}^{\infty} F_m \cos\frac{m\pi X}{aL} \qquad Y = \pm L/2 \tag{2}$$

$$M_Y = \sum_{m=1,3,\ldots}^{\infty} G_m \cos\frac{m\pi X}{L} \qquad Y = \pm L/2$$

where the coefficients E_m, F_m and G_m, $m = 1, 3, 5, \ldots$, remain to be determined. The dimension of these coefficients is moment per length.

Plate deflection solutions

By virtue of the small deflection assumption, we require that the edges of the box under load will remain straight and rotate only as a rigid connection. This simplification thus enables a closed form solution for each plate in terms of the unknown moment coefficients E_m, F_m and G_m. The differential equation governing the deflection of a typical plate has the form

$$D_{11}w_{,XXXX} + 2(D_{12} + 2D_{66})w_{,XXYY} + P_X w_{,XX} + P_Y w_{,YY} + D_{22}w_{,YYYY} = q. \tag{3}$$

For each plate, we employ a superposition scheme as depicted in Fig. 4. The total solution of a typical plate will then consist of the algebraic sum of three individual solutions due respectively to the pressure q, the edge moments parallel to X-axis and the edge moments parallel to Y-axis. Each individual solution is obtained by solving equation (3) with a Levy type single series method [5] and satisfying some appropriate boundary conditions.

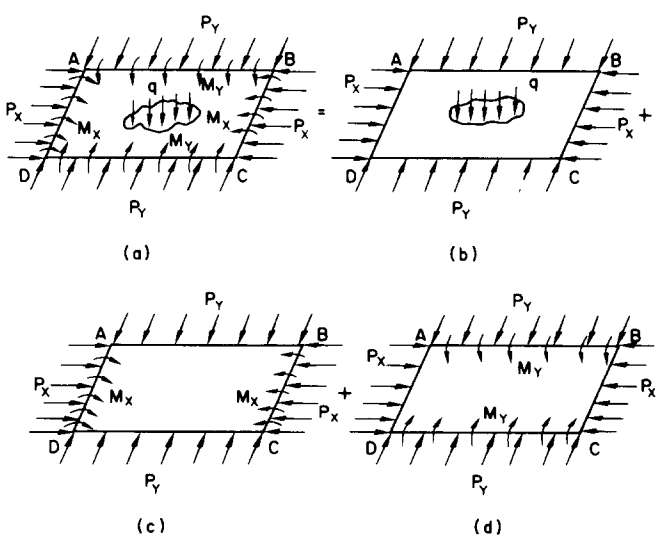

FIG. 4. Scheme of superposition.

To avoid too many technicalities however, we shall simply present the final expression of the plate deflection function for the top, side and front plates, respectively:

$$w_t = \frac{4qL^2b^4}{D^t_{11}} \sum \frac{(-1)^{(m-1)/2}\cos(n\pi x/b)}{m^3\pi^3(m^2\pi^2 - b^2 p_{xt})}\left[1 - \frac{u^2_{mt}\,\mathrm{Ch}(v_{mt}y)}{(u^2_{mt}-v^2_{mt})\,\mathrm{Ch}(v_{mt}/2)} + \frac{v^2_{mt}\,\mathrm{Ch}(u_{mt}y)}{(u^2_{mt}-v^2_{mt})\,\mathrm{Ch}(u_{mt}/2)}\right]$$

$$+ \frac{1}{qL}\sum \frac{(-1)^{(m-1)/2}E_m\cos(m\pi y)}{(\bar{u}^2_{mt}-\bar{v}^2_{mt})}\left[\frac{\mathrm{Ch}(\bar{v}_{mt}x)}{\mathrm{Ch}(\bar{v}_{mt}b)/2} - \frac{\mathrm{Ch}(\bar{u}_{mt}x)}{\mathrm{Ch}(\bar{u}_{mt}b)/2}\right]$$

$$+ \frac{D^t_{11}}{D^t_{22}qL}\sum \frac{(-1)^{(m-1)/2}G_m\cos(m\pi x/b)}{(u^2_{mt}-v^2_{mt})}\left[\frac{\mathrm{Ch}(v_{mt}y)}{\mathrm{Ch}(v_{mt}/2)} - \frac{\mathrm{Ch}(u_{mt}y)}{\mathrm{Ch}(u_{mt}/2)}\right] \tag{4}$$

$$w_s = \frac{4qL^2a^4}{D^s_{11}} \sum \frac{(-1)^{(m-1)/2}\cos(m\pi x/a)}{m^3\pi^3(m^2\pi^2 - a^2 p_{xs})}\left[1 - \frac{u^2_{ms}\,\mathrm{Ch}(v_{ms}y)}{(u^2_{ms}-v^2_{ms})\,\mathrm{Ch}(v_{ms}/2)} + \frac{v^2_{ms}\,\mathrm{Ch}(u_{ms}y)}{(u^2_{ms}-v^2_{ms})\,\mathrm{Ch}(u_{ms}/2)}\right]$$

$$+ \frac{D^t_{11}}{D^s_{11}qL}\sum \frac{(-1)^{(m-1)/2}E_m\cos(m\pi y)}{(\bar{u}^2_{ms}-\bar{v}^2_{ms})}\left[\frac{\mathrm{Ch}(\bar{v}_{ms}x)}{\mathrm{Ch}(\bar{v}_{ms}a/2)} - \frac{\mathrm{Ch}(\bar{u}_{ms}x)}{\mathrm{Ch}(\bar{u}_{ms}a/2)}\right]$$

$$+ \frac{D^t_{11}}{D^s_{11}qL}\sum \frac{(-1)^{(m-1)/2}F_m\cos(m\pi x/a)}{(u^2_{ms}-v^2_{ms})}\left[\frac{\mathrm{Ch}(v_{ms}y)}{\mathrm{Ch}(v_{ms}/2)} - \frac{\mathrm{Ch}(u_{ms}y)}{\mathrm{Ch}(u_{ms}/2)}\right] \tag{5}$$

$$w_f = \frac{4qL^2b^4}{D^f_{11}} \sum \frac{(-1)^{(m-1)/2}\cos(m\pi x/b)}{m^3\pi^3(m^2\pi^2 - b^2 p_{xf})}\left[1 - \frac{u^2_{mf}\,\mathrm{Ch}(v_{mf}y)}{(u^2_{mf}-v^2_{mf})\,\mathrm{Ch}(v_{mf}a/2)} + \frac{v^2_{mf}\,\mathrm{Ch}(u_{mf}y)}{(u^2_{mf}-v^2_{mf})\,\mathrm{Ch}(u_{mf}a/2)}\right]$$

$$+ \frac{D^t_{11}}{D^f_{11}qL}\sum \frac{(-1)^{(m-1)/2}F_m\cos(m\pi y/a)}{(\bar{u}^2_{mf}-\bar{v}^2_{mf})}\left[\frac{\mathrm{Ch}(\bar{v}_{mf}x)}{\mathrm{Ch}(\bar{v}_{mf}b/2)} - \frac{\mathrm{Ch}(\bar{u}_{mf}x)}{\mathrm{Ch}(\bar{u}_{mf}b/2)}\right]$$

$$+ \frac{D^t_{11}}{D^f_{22}qL}\sum \frac{(-1)^{(m-1)/2}G_m\cos(m\pi x/b)}{(u^2_{mf}-v^2_{mf})}\left[\frac{\mathrm{Ch}(v_{mf}y)}{\mathrm{Ch}(v_{mf}a/2)} - \frac{\mathrm{Ch}(u_{mf}y)}{\mathrm{Ch}(u_{mf}a/2)}\right]. \tag{6}$$

In the above equations, the $\sum$ sign sums up for $m = 1, 3, 5, \ldots$ and

$$x = X/L \qquad y = Y/L$$

and

$$p_{xk} = P_{Xk}L^2/D^k_{11} \qquad p_{yk} = P_{Yk}L^2/D^k_{11} \qquad k = t, s, f \tag{7}$$

$$\left.\begin{matrix} u_{mk} \\ v_{mk} \end{matrix}\right\} = \{f^m_{1k} \pm [(f^m_{1k})^2 - f^m_{2k}]^{\frac{1}{2}}\}^{\frac{1}{2}}$$

$$k = t, s, f; m = 1, 3, 5, \ldots \tag{8}$$

$$\left.\begin{matrix} \bar{u}_{mk} \\ \bar{v}_{mk} \end{matrix}\right\} = \{\bar{f}^m_{1k} \pm [(\bar{f}^m_{1k})^2 - \bar{f}^m_{2k}]^{\frac{1}{2}}\}^{\frac{1}{2}}$$

in which $f^m_{1k}, f^m_{2k}, \bar{f}^m_{1k}$ and $\bar{f}^m_{2k}$ are constants involving material, geometrical and loading parameters. Their full expressions are given as

$$
\begin{aligned}
f^m_{1k} &= \frac{(D^k_{12}+2D^k_{66})m^2\pi^2}{D^k_{22}d^k} - \frac{1}{2}\frac{D^k_{11}}{D^k_{22}}p_{yk} \\
f^m_{2k} &= \frac{D^k_{11}m^2\pi^2}{D^k_{22}d^k}\left(\frac{m^2\pi^2}{d^k} - p_{xk}\right) \\
\bar{f}^m_{1k} &= \frac{(D^k_{12}+2D^k_{66})m^2\pi^2}{D^k_{11}\,\mathrm{e}^k} - \frac{1}{2}p_{xk} \\
\bar{f}^m_{2k} &= \frac{m^2\pi^2}{\mathrm{e}^k}\left(\frac{m^2\pi^2 D^k_{22}}{D^k_{11}\,\mathrm{e}^k} - p_{yk}\right)
\end{aligned}
\qquad k = t, s, f \tag{9}
$$

where

$$
\begin{aligned}
(d^t, d^s, d^f) &= (b^2, a^2, b^2) \\
(\mathrm{e}^t, \mathrm{e}^s, \mathrm{e}^f) &= (1, 1, a^2).
\end{aligned}
$$

Edge shear forces

The shear forces along the edges of any plate may be obtained from the deflection function of the same plate. For example, the shear forces along the edge parallel to Y-axis of the top panel and along the edge parallel to X-axis of the top panel are, respectively, given by:

$$
\begin{aligned}
V_{Xt} &= -\frac{1}{L^3}[D^t_{11}w_{t,xxx} + (D^t_{12}+2D^t_{66})w_{t,xyy}] \qquad \text{at } x = \pm b/2 \\
V_{Yt} &= -\frac{1}{L^3}[(D^t_{12}+2D^t_{66})w_{t,xxy} + D^t_{22}w_{t,yyy}] \qquad \text{at } y = \pm 1/2.
\end{aligned} \tag{10}
$$

Similar expressions for shears on the side and front panels may be obtained from w_s and w_f functions.

Matching conditions

When the total structure is considered, the requirement of rigid edge rotations yields the following conditions along edges BC, CD and Cf:

$$
\begin{aligned}
w_{t,x}(x = b/2) + w_{s,x}(x = a/2) &= 0 \\
w_{t,y}(y = 1/2) + w_{f,y}(y = a/2) &= 0 \\
w_{s,y}(y = 1/2) + w'_{f,y}(y = 1/2) &= 0
\end{aligned} \tag{11}
$$

where w'_f is the deflection function of the front plate $CDFG$ when referred to the alternative coordinates shown in Fig. 1(e). It is derived from the function w_f in (6) by exchanging x and y [with due regard to those terms involving x, y indices in the expressions in (8) and their subsequent definitions in (9)]. Thus, the first of (11) is a function of y and the second and the third of (11) are functions of x.

When the expressions for deflection (4)–(6) are substituted into (11), each of which can be arranged in the form of a vanishing series,

$$f(t) = \sum_{m=1,3,\ldots}^{\infty} C_m \cos mt = 0.$$

And, for every $m = 1, 3, 5, \ldots$ we set the coefficient C_m to zero; we obtain the following set of algebraic equations:

$$\begin{aligned}
&\alpha_i E_i + \sum_{m=1,3,\ldots}^{\infty} \alpha_{im} E_m + \sum_{m=1,3,\ldots}^{\infty} \alpha'_{im} G_m = \alpha'_i q L^2 \\
&\sum_{m=1,3,\ldots}^{\infty} \beta_{im} E_m + \sum_{m=1,3,\ldots}^{\infty} \beta'_{im} F_m + \beta_i G_i = \beta'_i q L^2 \\
&\sum_{m=1,3,\ldots}^{\infty} \gamma_{im} E_m + \gamma_i F_i + \sum_{m=1,3,\ldots}^{\infty} \gamma'_{im} G_m = \gamma'_i q L^2.
\end{aligned} \tag{12}$$

The constants associated with E_i, F_i and G_i are dependent upon the material, geometric and loading parameters of the structure, and their full expressions are given in the Appendix.

Remarks on the convergence of solutions

For numerical solutions of the problem, the moment series as presented in (2) must be truncated at a finite number of terms, say N. Then, for $i = 1, 3, 5, \ldots (2N-1)$, equations (12) reduce to a set of $3N$ simultaneous equations in the unknowns E_i, F_i and G_i. The solutions of these are used in the calculation of the edge moments according to (2), of the plate deflections according to (4)–(6) and of the edge shears according to (10), etc.

As in many a series method, the question regarding the convergence of solutions arises in the present study as well. However, a rigorous proof of the convergence of the general system (12) did not seem to be accessible. Instead, two measures were taken in the present study to investigate at least partially the convergence nature of the solution scheme.† First, we simply truncated the series at different numbers of terms (we studied the cases for $N = 4$, 5, 8, 10 and 15), and examined numerically the solutions for each value of N. Almost in all cases computed, a convergence is believed to have been reached at $N = 8$ (when compared with the solutions for $N = 15$ the differences fall within 1 per cent).

In a second measure, we have considered a cubic box made of isotropic panels. In this case, because of symmetry $E_i = F_i = G_i$ for all i and the system (12) reduces simply to

$$E_i = \sum_{m=1,3,\ldots}^{\infty} \alpha_{im} E_m + \gamma_i, \qquad i = 1, 3, 5, \ldots. \tag{13}$$

According to a theory presented by Kantorovich and Krylov [6], the regularity of the system (13) will assure that the solution scheme presented here yields results converging to the exact solutions as $N \to \infty$. The regularity condition requires that

$$\sum_{m=1,3,\ldots}^{\infty} |\alpha_{im}| < 1, \qquad i = 1, 3, 5, \ldots. \tag{14}$$

† A detail discussion on this topic is included in [4].

Again, the inequality (14) was tested for a number of cases with i, m up to a value of 30. The inequality was satisfied for all values of pressure q below q_{cr}, the lowest critical pressure that the box can sustain.

NUMERICAL RESULTS AND DISCUSSIONS

In this section we shall present some numerical results and discuss certain unique characteristics of the box structure. The numerical work reported here was carried out on an IBM 360-75 computer; and all series were truncated after their 10th term ($N = 10$).

Multi-degree of freedom and buckling of box

When the box is placed under external pressure, each panel plate is subjected to a combined in-plane compression and out-of-plane bending. This action causes a decrease of structural rigidity under increasing load, a phenomenon analogous to some extent to the well known behavior of a beam-column. But the box is made of multiple panels and it therefore has many degrees of freedom in deflection. While according to the present theory, a given box will deflect and fail only in a single mode under increasing pressure, one must decide whether the calculated deflection represents the weakest possible deflected configuration. To do this, we consider first the buckling problem of the box. Briefly, we remove the total pressure load from each panel of the box and replace it with statically equivalent linear forces acting on all edges of the panel. An example showing such a replacement is given in Fig. 5. When this is done, the first term in each of equations (4)–(6) will vanish and the right-hand side of equations (12) drops out as a result. For non-trivial solutions for E_i, F_i and G_i, we require the vanishing of the determinant of the coefficient matrix and seek the proper values for the intensity of the linear forces (which contain the pressure q). Since the determinant presents a transcendental equation, it possesses a finite number of roots, the lowest of which corresponds physically to the first buckling pressure.

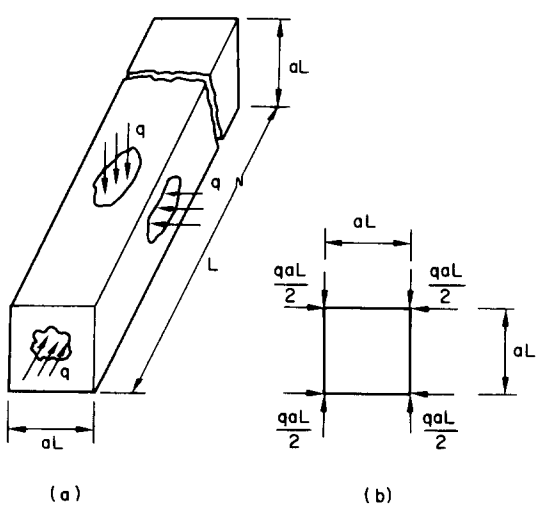

FIG. 5. Diagrams showing replacement of pressure to concentrated linear forces along edges of box.

For illustration, let us consider a cubic box made of six identical isotropic square plates. Following the procedure just outlined, the first four proper values of the linear forces, translated in q, are 95·75 D_{11}/L^3, 119·16 D_{11}/L^3, 210·52 D_{11}/L^3 and 407·50 D_{11}/L^3. Note that the buckling load for a clamped square plate under uniform bi-directional compression when expressed in q, is 210·52 D_{11}/L^3 (see [7]), which coincides with the third lowest buckling pressure of the box.

Perturbation of symmetry

We now return to the regular solution procedures that provide field solutions for the box at any loading stage before failure. In particular, if the box possesses a certain symmetry and if this symmetry is slightly perturbed, the resulting deflection of the box may be significantly altered. For example, consider again the isotropic cubic box. Ideally, the sides of the box may be represented by $L \times L \times L$. Because of a total symmetry with respect to the center of the box, all panel plates will deflect equally and inwardly under increasing pressure. Hence, each panel behaves as a clamped square plate. Curve 3 in Fig. 6 shows the center-panel deflection (in qL^4/D_{11}) against the pressure (in D_{11}/L^3). Observe that the curve starts out horizontally from zero pressure and remains fairly flat when the pressure is small. This indicates the insignificant effect of the in-plane compression in the solutions and the

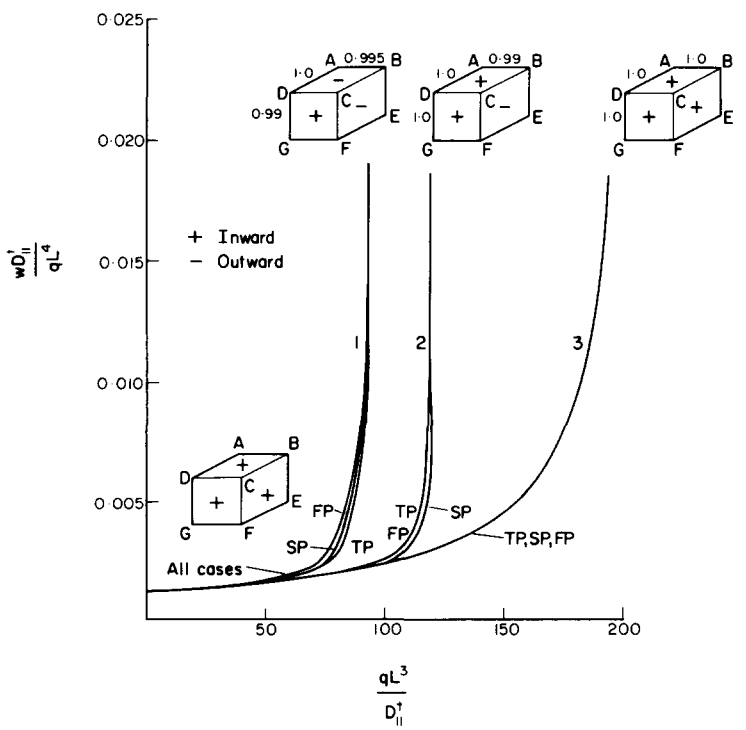

Fig. 6. Deflections at center of panels of a cubic box vs. pressure intensity.

proportionality between the deflection and the intensity of q.† As the pressure increases, the curve bends up dramatically, indicating a nonlinear behavior as a result of the combined bending–compression action. A limiting pressure exists at which the structure will probably fail because of excessive panel deflection. The limiting pressure for this ideal cubic box is found to be $210{\cdot}52\ D_{11}/L^3$ which compares with the third buckling pressure of this box.

When the geometrical symmetry of the cubic box is perturbed, say be making the dimensions of the cube to $L \times L \times 0{\cdot}995L$, the limiting pressure in this case is $119{\cdot}16\ D_{11}/L^3$ (see curve 2, Fig. 6). Similarly, by further relaxing the symmetry, say by making the cube to $L \times 0{\cdot}99L \times 0{\cdot}995L$, the resulting ultimate pressure reduces to merely $95{\cdot}75\ D_{11}/L^3$, curve 1. A close study of Fig. 6 will also show that in all the three cases just mentioned, the panel deflections follow essentially the same single curve with all panels deflected almost equally and inwardly at the beginning of the pressure stage. However, when the pressure is substantially increased, the fully perturbed box (curve 1) starts to undergo large deflections and simultaneously two pairs of its panels pop out prior to reaching its limiting pressure. The reversion of deflection at this point is apparently caused by uneven edge rotations as a result of the perturbation of symmetry. In the case of the partially perturbed box (curve 2), only one pair of panels pops out before reaching the limiting pressure, which is higher than in the first case. The presence of ideal symmetry is thus seen to dictate the mode shape and effectively strengthens the structure's rigidity. In the same light, we see for the cubic box that the assumed perfect symmetry has resulted the box to deflect in its third mode shape and the corresponding limiting pressure was more than twice its first (lowest) critical pressure. Since ideal symmetry does not exist in practice, it is therefore essential to determine the lowest mode of failure.

Orthotropic reinforcements

When all box panels, or some of them, are reinforced with ribs, sandwich core or fibrous materials in such a way that their over-all elastic properties are describable by an orthotropic plate, then the present analysis provides solutions for such structures. The translation of material properties from a reinforced plate to one which is homogeneous and orthotropic has been extensively discussed in the literature, see e.g. [2, 3].

In the following two examples, we shall illustrate the effect of orthotropy on the behavior of the boxes.

Case 1. Cubic box reinforced with orthogonal ribs on all panels such that

$$D_{11}^k = D_{22}^k = 2(D_{12}^k + 2D_{66}^k) = 2D_0, \qquad k = t, s, f,$$

where D_0 is the flexural rigidity of the panels without reinforcement. By doubling the rigidities D_{11} and D_{22} on all panels, the critical first mode failure occurred at a pressure which is 1·75 times that at which it occurred when without reinforcement.

Case 2. A square based box of dimension $L \times \frac{1}{2}L \times L$. When without reinforcement, the first critical pressure is found to be $113{\cdot}8\ D_0/L^3$. If only the weaker top and bottom panels are reinforced by orthogonal ribs such that

$$D_{11}^t = D_{22}^t = 2(D_{12}^t + 2D_{66}^t) = 2D_0$$

$$D_{11}^k = D_{22}^k = 2(D_{12}^k + 2D_{66}^k) = D_0, \qquad k = s, f,$$

† For small q, the results here agree well with those obtained by Conway [1], who did not consider effects of in-plane forces.

then the resulting first critical pressure is 219·52 D_0/L^3. When, in addition, the four side panels are reinforced in the weaker direction (parallel to the longer edge), such that

$$D^s_{11} = D^f_{22} = 2D_0$$

$$D^s_{22} = D^f_{11} = (D^s_{12} + 2D^s_{66}) = (D^f_{12} + 2D^f_{66}) = D_0$$

the first critical pressure is increased to 275·14 D_0/L^3. This represents more than $2\frac{1}{2}$ times improvement in the strength over the original isotropic box.

Long rectangular boxes

The strength of long, thin-walled boxes subjected to compressive loads has customarily been treated using the well known theory of polygonal shells (see e.g. [7]). The question arises, however, as to at what length of a box it is considered long. A partial answer to this question may be rendered from the present results. For the purpose of a comparison, consider two boxes, both made of isotropic panels, having the respective dimensions of $1 \times 0{\cdot}2 \times 0{\cdot}2L^3$ and $1 \times 0{\cdot}5 \times 0{\cdot}5L^3$. The two boxes are first analyzed for their buckling pressure according to the present method and the results are then compared with those obtained according to the "long" box approximation (see [7, pp. 62–64]). The following table contains the respective lowest buckling strength:

TABLE 1

Box size (L^3)	Present analysis	Long box analysis
$1 \times 0{\cdot}2 \times 0{\cdot}2$	2590 D/L^3	2500 D/L^3
$1 \times 0{\cdot}5 \times 0{\cdot}5$	329 D/L^3	160 D/L^3

It may be concluded that a box (of isotropic panels) may be considered "long" when its longitudinal dimension is five times or more larger than its transverse dimensions. Clearly, the definition of a long box of orthotropic panels depends on the degree of orthotropy of each pair of its panels.

CONCLUDING REMARKS

The strength and stability of orthotropic, rectangular boxes subjected to external pressure are analyzed here. The method used is based on the well known theory of linearly elastic plates. The various deflected modes of the boxes under pressure are determined by means of a scheme of geometric perturbation, which leads to the determination of the corresponding mode of buckling strength of the structures.

It is found that a proper choice of the physical dimension of the box or an adequate reinforcement of the box, or both, will significantly increase the structure's rigidity. While it is realized that one cannot exhaust all possible material and/or geometrical combinations of the box so as to obtain the strongest and perhaps the most economical structure, the present analysis does suggest a possibility that a most advantageous design may be achieved. Such a possibility will be explored in future studies, however.

It will be noted that, by reversing the sign of q, we can immediately obtain results for boxes pressurized from within. Furthermore, although the present analysis requires the

external pressure to be uniform, the solution procedure illustrated herein may be readily applied to cases in which loadings are not uniformly distributed, but are nevertheless self-equilibrating. Of course, the underlying assumption that the edges of the box remain straight and underformed throughout the loading history must not be violated. This restriction will be likely to exclude loading conditions that cause twisting of the boxes. In such cases, and for boxes of "medium" lengths (i.e. by using long-box approximation), one may make use of the variational approach introduced by Vlasov [8, Parts IV and V] (see also [9]). Satisfactory results for arbitrarily loaded general boxes, however, have yet to be obtained.

Acknowledgments—The authors wish to thank the reviewers for their comments and their bringing to the authors' attention Refs. [8, 9].

REFERENCES

[1] H. D. Conway, Stresses in a pressurized box. *J. Struct. Div. Am. Soc. civ. Engrs* **89**, 95–105 (1963).
[2] S. G. Lekhnitskii, *Anisotropic Plates*, p. 373. Gordon and Breach (1958).
[3] J. E. Ashton and J. M. Whitney, *Theory of Laminated Plates*, pp. 45–76. Technomic (1970).
[4] J. R. Yalakki, Strength and Stability of Box Structures Subject to Compressive Loads, Dissertation, Drexel University (1971).
[5] M. Levy, Sur l'equilibre élastique d'une plaque rectangulaire. *C. r. hebd. Séanc. Acad. Sci., Paris* **129**, 535–539 (1899).
[6] L. V. Kantorovich and V. I. Krylov, *Approximate Methods of Higher Analysis*, pp. 1–77. Interscience (1958).
[7] S. P. Timoshenko and J. M. Gere, *Theory of Elastic Stability*, pp. 351–389. McGraw-Hill (1961).
[8] V. Z. Vlasov, General Theory of Shells and Its Applications in Engineering, NASA TT-F-99, pp. 544–714 (1964).
[9] I. F. Obrazcov, *Variational Methods of Analysis of Thin-Walled Aircraft Structures*, (in Russian). Moscow (1966).

APPENDIX

The constants that appear in equations (12) are defined as:

$$\alpha_i = \frac{1}{\bar{u}_{it}^2 - \bar{v}_{it}^2}\left(\bar{u}_{it}\mathrm{Th}\frac{\bar{u}_{it}b}{2} - \bar{v}_{it}\mathrm{Th}\frac{\bar{v}_{it}b}{2}\right) + \frac{D^t_{11}}{D^s_{11}(\bar{u}_{is}^2 - \bar{v}_{is}^2)}\left(\bar{u}_{is}\mathrm{Th}\frac{\bar{u}_{is}a}{2} - \bar{v}_{is}\mathrm{Th}\frac{\bar{v}_{is}a}{2}\right)\Bigg]$$

$$\alpha_{im} = \frac{D^t_{11}(4\pi^2 im)}{D^s_{22}a(i^2\pi^2 + u_{ms}^2)(i^2\pi^2 + v_{ms}^2)}$$

$$\alpha'_{im} = \frac{D^t_{11}(4\pi^2 im)}{D^t_{22}b(i^2\pi^2 + u_{mt}^2)(i^2\pi^2 + v_{mt}^2)}$$

$$\alpha'_i = \frac{4qL^3}{i^3\pi^3}\Bigg[\frac{\bar{u}_{it}\bar{v}_{it}}{(\bar{u}_{it}^2 - \bar{v}_{it}^2)(D^s_{22}i^2\pi^2 - D^t_{11}p_{yt})}\left(\bar{v}_{it}\mathrm{Th}\frac{\bar{u}_{it}b}{2} - \bar{u}_{it}\mathrm{Th}\frac{\bar{v}_{it}b}{2}\right)$$

$$+ \frac{\bar{u}_{is}\bar{v}_{is}D^s_{11}/D^t_{11}}{(\bar{u}_{is}^2 - \bar{v}_{is}^2)(D^s_{22}i^2\pi^2 - D^t_{11}p_{ys})}\left(\bar{v}_{is}\mathrm{Th}\frac{\bar{u}_{is}a}{2} - \bar{u}_{is}\mathrm{Th}\frac{\bar{v}_{is}a}{2}\right)\Bigg]$$

$$\beta_i = \frac{D^t_{11}/D^t_{22}}{(u^2-v^2_{is})}\left(u_{is}\mathrm{Th}\frac{u_{is}}{2}-v_{is}\mathrm{Th}\frac{v_{is}}{2}\right)+\frac{D^t_{11}/D^f_{11}}{(\bar{u}'^2_{if}-\bar{v}'^2_{if})}\left(\bar{u}'_{if}\mathrm{Th}\frac{\bar{u}'_{if}b}{2}-\bar{v}'_{if}\mathrm{Th}\frac{\bar{v}'_{if}b}{2}\right)\Bigg]$$

$$\beta_{im} = \frac{D^t_{11}(4\pi^2a^2im)}{D^s_{11}(i^2\pi^2+a^2\bar{u}^2_{ms})(i^2\pi^2+\bar{v}^2_{ms}a^2)}$$

$$\beta'_{im} = \frac{D^t_{11}(4\pi^2a^2im)}{D^f_{22}b(i^2\pi^2+a^2u'^2_{mf})(i^2\pi^2+a^2v'^2_{mf})}$$

$$\beta'_i = \frac{4qL^3a^4}{i^3\pi^3}\Bigg[\frac{\bar{u}'_{if}\bar{v}'_{if}}{(\bar{u}'^2_{if}-\bar{v}'^2_{if})(D^f_{22}i^2\pi^2-D^f_{11}a^2p_{yf})}\left(\bar{v}'_{if}\mathrm{Th}\frac{\bar{u}'_{if}b}{2}-\bar{u}'_{if}\mathrm{Th}\frac{\bar{v}'_{if}b}{2}\right)$$

$$+\frac{u_{is}v_{is}}{D^s_{11}(u^2_{is}-v^2_{is})(i^2\pi^2-a^2p_{xs})}\left(v_{is}\mathrm{Th}\frac{u_{is}}{2}-u_{is}\mathrm{Th}\frac{v_{is}}{2}\right)\Bigg]$$

$$\gamma_i = \left[\frac{D^t_{11}/D^t_{22}}{(u^2_{it}-\bar{v}^2_{it})}\left(u_{it}\mathrm{Th}\frac{u_{it}}{2}-v_{it}\mathrm{Th}\frac{v_{it}}{2}\right)+\frac{D^t_{11}/D^f_{22}}{(u^2_{if}-v^2_{if})}\left(u_{if}\mathrm{Th}\frac{u_{if}a}{2}-v_{if}\mathrm{Th}\frac{v_{if}a}{2}\right)\right]$$

$$\gamma_{im} = \frac{4\pi^2b^2im}{(i^2\pi^2+b^2\bar{u}^2_{mt})(i^2\pi^2+b^2\bar{v}^2_{mt})}$$

$$\gamma'_{im} = \frac{D^t_{11}(4\pi^2b^2im)}{D^f_{11}a(i^2\pi^2+b^2\bar{u}^2_{mf})(i^2\pi^2+b^2\bar{v}^2_{mf})}$$

$$\gamma'_i = \frac{4qL^3b^4}{i^3\pi^3}\Bigg[\frac{u_{it}v_{it}}{D^t_{11}(u^2_{it}-v^2_{it})(i^2\pi^2-b^2p_{xt})}\left(v_{it}\mathrm{Th}\frac{u_{it}}{2}-u_{it}\mathrm{Th}\frac{v_{it}}{2}\right)$$

$$+\frac{u_{if}v_{if}}{D^f_{11}(u^2_{if}-v^2_{if})(i^2\pi^2-b^2p_{xf})}\left(v_{if}\mathrm{Th}\frac{u_{if}a}{2}-u_{if}\mathrm{Th}\frac{v_{if}a}{2}\right)\Bigg].$$

In the above expressions, the symbols u'_{if}, v'_{if}, $\bar{u}'_{if}$ and $\bar{v}'_{if}$ are equivalent to u_{if}, v_{if}, $\bar{u}_{if}$ and $\bar{v}_{if}$, respectively, when in each the subscript x is replaced by y and vice versa. See the definitions in equations (8) and (9).

(*Received* 7 *September* 1971; *revised* 28 *October* 1971)

Абстракт—На основе классической теории пластинок, дается анализ упругих напряжений прогибов критических давлений, для рахных видов разрушения прямоугольной коробки, подверженной действию поля равномерного внешнего давления. С помощью схемы наложения и метода разложения в одинарные ряды, решаются уравнения поля, описывающие прогиб ортотропной пластинки. Дается полное решение для целой коробки, путем наложения непрерывности на краях, где находятся отдельные пластинки. Представленный, здесь, метод анализа можно применить к коробкам, для которых внешние, сжимающие давления равномерны, но само-равновесные.